Role of the Aerosol Substrate in the Heterogeneous Ozonation Reactions of Surface-Bound PAHs

N.-O. A. Kwamena, M. G. Staikova, D. J. Donaldson, I. J. George, and J. P. D. Abbatt*

Department of Chemistry, University of Toronto, Ontario, Canada M5S 3H6

Received: July 7, 2007; In Final Form: August 20, 2007

To probe how the aerosol substrate influences heterogeneous polycyclic aromatic hydrocarbon (PAH) oxidation, we investigated the reaction of surface-bound anthracene with gas-phase ozone on phenylsiloxane oil and azelaic acid aerosols under dry conditions in an aerosol flow tube with offline analysis of anthracene. The reaction exhibited pseudo-first-order kinetics for anthracene loss, and the pseudo-first-order rate coefficients displayed a Langmuir−Hinshelwood dependence on the gas-phase ozone concentration on both aerosol substrates. The following parameters were found: for the reaction on phenylsiloxane oil aerosols, $K_{O_3} = (1.0 \pm 0.4) \times 10^{-13}$ cm^3 and $k^{I}_{max} = (0.010 \pm 0.003)$ s^{-1}; for the reaction on azelaic acid aerosols, $K_{O_3} = (2.2 \pm 0.9) \times 10^{-15}$ cm^3 and $k^{I}_{max} = (0.057 \pm 0.009)$ s^{-1}, where K_{O_3} is a parameter that describes the partitioning of ozone to the surface and k^{I}_{max} is the maximum pseudo-first-order rate coefficient at high ozone concentrations. The K_{O_3} value for the reaction of surface-bound anthracene and ozone on azelaic acid aerosols is similar to the K_{O_3} value that we obtained in our previous study for the reaction of surface-bound benzo[*a*]pyrene and ozone on the same substrate. This finding supports our earlier hypothesis that the substrate influences the partitioning of ozone to the surface irrespective of the organic species (i.e., PAH) adsorbed to it. Preliminary ab initio calculations were performed to investigate whether there is a relationship between the relative binding energies of the ozone−substrate complex and the K_{O_3} values for the different substrates studied. A comparison between kinetic results obtained on aerosol substrates and thin films is presented.

1. Introduction

The reactive fate of a chemical in the troposphere is governed by both gas-phase and heterogeneous chemistry. The relative importance of gas-phase versus heterogeneous chemistry depends on the vapor pressure of the chemical in question; heterogeneous chemistry is particularly important for species of lower volatility that partition to atmospheric particulate matter. In addition, the reaction may be more efficient in or on condensed matter than in the gas phase. Therefore, to better understand the factors that govern heterogeneous chemistry, we investigated the reaction of surface-bound polycyclic aromatic hydrocarbons (PAHs) and ozone (O_3) on different aerosol substrates.

Organic compounds, including PAHs, dicarboxylic acids, and other highly oxygenated compounds, are the second most abundant class of compounds after sulfate and nitrates in particles <1 μm in size.[1,2] PAHs in particular receive considerable research attention because they are carcinogenic, mutagenic, and allergenic in nature. It has been long understood that the reactive fate of volatile PAHs, such as naphthalene, is governed by gas-phase reactions with the hydroxyl radical.[3,4] However, heavier PAHs such as benzo[*a*]pyrene (BaP) are found sorbed on particulate matter and other surfaces, and therefore heterogeneous oxidation and nitration reactions with atmospheric oxidants are their primary sinks.[4] Recent laboratory studies on aerosol substrates,[5,6] at the air−aqueous interface,[7,8] on surface films,[9] and using a coated-wall flow tube apparatus[10] suggest that heterogeneous reactions may be more important than their corresponding gas-phase reactions as sinks for these compounds. A recent modeling study has shown that, under certain conditions in the urban environment, these heterogeneous reactions may be the dominant reactive loss process.[11]

To understand how the heterogeneous loss of PAHs and atmospheric oxidants proceeds, it is important to determine the reaction mechanism and the factors that might influence it. These include the nature of the substrate, the type of oxidant, and environmental conditions such as light and relative humidity. Work by Alebic-Juretic et al.[12] and Wu et al.[13] looked at the heterogeneous reaction of surface-bound BaP and ozone and revealed a linear dependence of the observed first-order rate coefficients with gas-phase ozone concentration. This linear dependence suggests a simple bimolecular reaction between the surface-adsorbed BaP and gas-phase ozone typical of an Eley−Rideal gas−surface reaction mechanism.[14]

In contrast, more recent laboratory studies investigating the reaction of surface-bound BaP and ozone by Pöschl et al.[5] on soot aerosols and by Kwamena et al.[6] on azelaic acid aerosols show a nonlinear dependence of the pseudo-first-order rate constant as a function of ozone concentration, typical of reactions that proceed by the Langmuir−Hinshelwood mechanism. The Langmuir−Hinshelwood mechanism has also been observed by Mmereki and co-workers[7,8] for the reaction of ozone and anthracene adsorbed to different coated aqueous surfaces and by Kahan et al.[9] for the reaction of ozone with a suite of six PAHs (naphthalene, fluoranthene, anthracene, phenanthrene, pyrene, and BaP) sorbed to 1-octanol. A reaction occurring by this mechanism implies that one reactant (i.e., the PAH) is adsorbed to the particle surface and the second reactant (i.e., ozone) is distributed between the gas and sorbed phases at equilibrium. There are two parameters that characterize the

* Corresponding author. Fax: (416) 946-7359. E-mail: jabbatt@chem.utoronto.ca.

10.1021/jp075300i CCC: $37.00
Published on Web 10/10/2007

Langmuir−Hinshelwood mechanism: the ozone partition coefficient (K_{O_3}), which describes the partitioning of ozone to the surface, and the maximum pseudo-first-order rate coefficient (k^{I}_{max}), which describes the surface reaction rate constant at high ozone concentrations, where the surface becomes saturated with this reactant.

In our previous study,[6] we investigated the heterogeneous reaction between surface-bound BaP and ozone on liquid azelaic acid aerosols and solid sodium chloride aerosols under both dry and high relative humidity conditions. We compared our results to those obtained on soot aerosols by Pöschl et al.[5] and suggested that the greatest influence of the aerosol substrate on the kinetics is controlling the partitioning of the ozone to the surface. Following that study we also investigated the heterogeneous reaction of gas-phase ozone with anthracene on coated Pyrex tubes,[15] a proxy for an inert, solid aerosol substrate.

The aim of the present study is to further explore the role of the aerosol substrate in affecting the kinetics of surface-bound PAHs and ozone on different aerosol surfaces. We were motivated to perform our studies on aerosols with diameters of less than 200 nm in order to reduce the influence of condensed-phase diffusion on the kinetics of the surface reaction. We also performed a small number of experiments on thin films using a laser-induced-fluorescence approach in order to compare the kinetics observed on particles to those on thicker substrates. We first investigated the reaction of surface-bound anthracene and ozone on azelaic acid aerosols to complement our earlier study using the same aerosol substrate. Our hypothesis was that if the substrate is governing the partitioning of ozone to the surface then the K_{O_3} value should not depend on the PAH that is being investigated, and we would observe K_{O_3} values for our current study investigating the reaction of surface-bound anthracene and ozone on azelaic acid aerosols similar to those we obtained for our study looking at the reaction of surface-bound BaP and ozone on azelaic acid. We also studied the reaction of surface-bound anthracene and ozone on phenylsiloxane oil aerosols to see if we would observe the same Langmuir−Hinshelwood behavior using a different substrate. Phenylsiloxane oil, which is made up of phenyl and methyl groups, is quite hydrophobic, therefore making it chemically different from azelaic acid. Finally, ab initio calculations were used to help explain the differing partitioning behavior of ozone toward the aerosol and thin film surfaces that have been used.

2. Experimental Section

2.1. Aerosol Generation and Coating. We used a previously developed kinetic approach to investigate the reaction between ozone and PAHs adsorbed to different aerosol surfaces.[5,6] Aerosols, generated by homogeneous nucleation, were coated with submonolayers of anthracene and exposed to ozone for different reaction times in a vertically oriented aerosol flow tube. The aerosols were then collected on filter paper and offline extraction and analysis techniques were used to determine the kinetics by determining the amount of anthracene remaining after ozone exposure. Details of the experimental approach are given below.

Azelaic acid and phenylsiloxane oil aerosols were chosen as model liquid aerosols because these two compounds should have little reactivity with ozone. The phenylsiloxane oil that was used was a 1,1,5,5-tetraphenyltetramethyltrisiloxane. Given the structure of the pump oil, there are no functional groups that should react with ozone. To support this, we saw no reactive loss of ozone upon exposure to this oil during low-pressure, coated-wall flow tube experiments. Saturated dicarboxylic acids are also not expected to exhibit reactivity toward ozone. Azelaic acid and phenylsiloxane oil aerosols were both generated by homogeneous nucleation. A mass flow controller (MKS Inc.) was used to send a volumetric flow of 0.3 lpm (liters per minute) N_2 through a 30.5 cm Pyrex tube containing azelaic acid (98%, Sigma Aldrich) or phenylsiloxane oil (Varian Inc.). The flow then passed through a heated region containing anthracene to coat the particles. The anthracene fractional surface coverage was controlled by adjusting the temperature of the anthracene coating region. All kinetic experiments were run with the following conditions: anthracene coating region temperature $T_{anthracene} = 318$ K, flow tube temperature of 298 ± 5 K, and particle number density in the flow tube of approximately 10^5 cm^{-3}. The median diameter of the aerosols was approximately 175 and 145 nm for phenylsiloxane oil aerosols and azelaic acid aerosols, respectively, with a geometric standard deviation of $\sigma_d = 1.4$.

2.2. Aerosol Flow Reactor. Dry N_2 (1.5 lpm) was added using a mass flow meter (MKS Inc.) to make the total flow through the vertically oriented Pyrex aerosol flow tube (inside diameter 6 cm, length 96 cm) 1.9 lpm. The aerosol flow tube was operated under laminar flow conditions at ambient pressure and temperature (1 atm, 298 K). Ozone was generated by ultraviolet irradiation of a mixed flow (total flow ~0.09 lpm) of O_2 and N_2 by a mercury pen lamp (length 22.5 cm; UVP Inc.) in a homemade Pyrex glass chamber. The ozone concentration was controlled by varying the ratio of O_2 to N_2 passing over the Pen-Ray lamp. Ozone was detected using a second mercury Pen-Ray lamp (length 5.3 cm; UVP Inc) placed in front of a homemade 10.3-cm-long or 50-cm-long absorbance cell with quartz windows at either end. An interference filter (Esco Products) was placed in front of an ultraviolet-sensitive photodiode (Boston Electronics Corp.) at the other end of the absorbance cell to determine the ozone concentration entering the aerosol flow tube. Ozone was introduced through a moveable Pyrex rod injector, which split into four prongs at the end to facilitate rapid mixing of the ozone into the total flow. The reaction time (up to 80 s) between ozone and surface-bound anthracene, which was varied by setting the injector to different positions along the length of the flow tube, was calculated from the bulk flow velocity. The maximum correction to the pseudo-first-order rate coefficient from the plug flow approximation was 4%, as based on the model of Brown.[16]

The reaction between anthracene and ozone was stopped by using an ozone denuder positioned immediately after the flow tube. Following the denuder, part of the aerosol flow (1.5 lpm) was diverted to a glass fiber filter (GF/A 47 mm, Whatman), which was mounted on a homemade stainless steel filter holder, for aerosol collection. Aerosols were collected for 6.5 min. Duplicate filter samples were taken at six different injector sampling positions between 0 and 86 cm. The error for each point was determined by taking the variability in the replicate measurements at each injector position. This flow was then vented into the laboratory's main exhaust line. The remaining aerosol flow was sent to a differential mobility analyzer (DMA; TSI Inc., Model 3080) connected to a condensation particle counter (CPC; TSI Inc., Model 3010) to monitor the aerosol size distributions. The DMA/CPC measurements were obtained simultaneously with the aerosol filter collection.

2.3. Aerosol Sampling and Analytical Methods. The kinetics were determined by monitoring the amount of unreacted anthracene on the aerosols after exposure to ozone at each injector position. Following collection, the filters were stored at 277 K until analysis. The filters were ultrasonically extracted

twice with dichloromethane (99.9% HPLC grade, Sigma-Aldrich). The extracts were evaporated to dryness under a gentle stream of nitrogen gas, reconstituted in 400 μL of acetonitrile (HPLC grade, Fisher Scientific) and analyzed by high-performance liquid chromatography (HPLC) with ultraviolet detection. A HPLC system from Waters (Waters 600 pump and controller) was interfaced to a diode array detector (Waters 996 photodiode array detector) and an autosampler (Waters 717 plus autosampler). The system was equipped with a C-18 guard column (Gemini, 4.0 × 2.0 mm, Phenomenex) coupled to a C-18 reversed-phase chromatographic column (Gemini, 150 mm × 2.00 mm × 5 μm, Phenomenex). Analysis was performed using a 10 μL injection volume and an isocratic elution of acetonitrile−water (70:30 v/v, HPLC-grade, Fisher Scientific, and 18 MΩ water, respectively) at a constant flow rate of 0.5 mL min^{-1}. Absorbance at 254 nm was used to monitor the anthracene signal. The Millenium 32 software package (Waters) was used to integrate the chromatographic peaks. The degradation of anthracene was quantified using an external standards calibration of anthracene standard solutions ranging from a few parts per billion to a few parts per million, which was run along with each kinetic analysis. Spike and recovery experiments on anthracene revealed an anthracene recovery of 70%. HPLC peak areas were corrected for 100% recovery before quantification with the calibration curve.

2.4. Fourier Transform Infrared (FTIR) Spectroscopy Experiments. In our work investigating the reaction of BaP and ozone on azelaic acid aerosols, we assumed that the azelaic acid aerosols were solid given that the melting point of azelaic acid is 106.5 °C and the experiment was conducted at room temperature.[6] However, recent work by Hearn and Smith[17] suggest that aerosols of this type may significantly supercool. An aerosol flow tube FTIR spectrometer apparatus was used to determine the phase of the aerosol and whether it changed by cooling or heating the aerosols or by the length of time they spend in the flow system. The experimental setup has been previously described.[18,19] The aerosol flow conditions described above were used for these experiments. Infrared spectra were obtained using a FTIR spectrometer (Bomen MB104) and an external MCT detector (Bomen). The path length of the flow tube was approximately 40 cm. The spectra were an average of 100 scans and were recorded over a wavenumber range of 4000−500 cm^{-1} at a resolution of 4 cm^{-1}.

2.5. Computational Approach. Density functional theory (DFT) calculations were performed as a preliminary means of addressing the differences in the K_{O_3} values for the different substrates investigated. The goal was to determine if there is a simple relationship between the experimentally determined K_{O_3} values and the ozone−organic substrate binding energies. The Gaussian 2003[20] suite of programs was used for all molecular calculations. The optimized geometries were calculated using Møller−Plesset perturbation theory (MP2) and the 6-31d basis set. DFT(B3LYP) using the 6-311++g(d,p) basis set was used to calculate the energies of the optimized geometries of the following complexes: azelaic acid−ozone, octanol−ozone, water−ozone, and benzene−ozone. These complexes represent the different substrates that have been used in studies of the heterogeneous reaction of surface-bound anthracene and ozone. The benzene−ozone complex was used to approximate the interaction of ozone with phenylsiloxane oil or soot given that both the soot and the phenylsiloxane oil are made of many benzene rings. Note that the goal was not to quantitatively estimate K_{O_3} values, which involve much more complex interactions than those included in a simple binary complex. Rather, we sought to see if the trend in the calculated binding energies could begin to explain the trend in the K_{O_3} values in the literature. In determining the energy of the complexes, an estimate of the basis set superposition error (BSSE) using the counterpoise method was included.[20]

2.6. Thin Film Kinetics Experiments. Laser-induced-fluorescence kinetic experiments were performed to compare the results on atmospheric aerosols with those on thin films. The details of the experimental procedure have been described elsewhere.[9] Briefly, 30 μL of phenylsiloxane oil was placed on a Pyrex microscope slide that had been smeared with a thin film of vacuum grease (Dow Corning silicone stopcock grease). The slide was placed in a ∼500 mL Teflon chamber, which had quartz windows at either end to allow a laser beam to enter and exit the chamber. Side ports in the chamber allowed introduction and ventilation of gases. A flow saturated with anthracene was used to deposit anthracene from the gas phase onto the phenylsiloxane oil thin film samples. Different deposition times, of 1 and 3 min, were used to vary the anthracene surface concentration. Ozone was generated and quantified using a method similar to that described in section 2.2. A pulsed frequency-tripled Nd:YAG laser (Minilite II, Continuum) with a repetition rate of 10 Hz and a maximum pulse energy of 4 mJ was used to excite the anthracene on the thin films. Anthracene was excited at 355 nm, and fluorescence, which was collected perpendicular to the sample, was detected at 404 nm.

The amount of anthracene on the phenylsiloxane oil thin film before and after exposure was quantified by placing glass fiber filters (GF/A 47 mm, Whatman) over the Pyrex microscope slide with the phenylsiloxane oil film to remove the film from the slide's surface. The filter paper was stored at 277 K until analysis. The samples were extracted using the same procedure that was used for the kinetic experiments (refer to section 2.3).

2.7. Chemicals. All chemicals were of reagent grade and used without further purification. Anthracene (99%) and azelaic acid (98%) were purchased from Sigma-Aldrich. Phenylsiloxane oil (DC-704, CAS Registry No. 3982-82-9) was purchased from Varian Inc. HPLC-grade dichloromethane and acetonitrile were obtained from Sigma-Aldrich and Fisher Scientific, respectively. Ultrahigh-purity N_2 and O_2 were obtained from BOC Gases Canada.

3. Results

3.1. Phase of the Organic Aerosol Substrates. In our initial work investigating the reaction of surface-bound PAHs and ozone, we performed our experiments using azelaic acid aerosols under the assumption that they were solid particles. However, recently, Hearn and Smith[17] investigated whether mixed oleic acid/myristic acid aerosols were solid or supercooled. They noted that the peak in their FTIR spectrum positioned at 1700 cm^{-1}, which is characteristic of the C═O stretch of carboxylic acids, was red shifted 9 cm^{-1} when the particles had been precooled compared to when the particles had only been exposed to room temperature. From characteristics in the FTIR spectrum, they believe the precooled aerosols had crystallized whereas those particles that had not been precooled had characteristics of liquid aerosols. We performed similar FTIR experiments and also looked at the characteristic peak at 1700 cm^{-1} to determine the phase of the azelaic acid aerosols.

As shown in Table 1, the peak at 1700 cm^{-1} was red shifted by approximately 10 cm^{-1} when the aerosols were precooled to 273 K prior to sampling with the FTIR; i.e., we believe this cooling process causes the particles to crystallize. In our kinetic

TABLE 1: Comparison of the Location of the C═O Stretch Peak for Azelaic Acid Aerosols under Different Experimental Conditions

aerosol conditions	location of the C═O stretch peak (cm^{-1})
aerosols sampled at room temperature (supercooled)	1710
aerosol precooled to 273 K and warmed to room temperature (solid particles)	1700
aerosols sent through a second heated region to simulate the anthracene coating process (supercooled)	1711
aerosols sent through flow tube used for kinetic studies (supercooled)	1711

studies we send the azelaic acid aerosols through a second heated region to coat them with anthracene before introduction into the aerosol flow tube where the anthracene-coated particles are then exposed to ozone. Therefore, for the FTIR experiments we sent the azelaic acid aerosols through a second heated region and through the flow tube to see if this had any effect on the phase of the particles. Table 1 shows that there was no shift in the position of the C═O peak as a result of heating or being sent through the flow tube, and therefore we conclude that the azelaic acid aerosols may be supercooled during our kinetic studies. We will, therefore, refer to the azelaic acid particles as liquid aerosols.

3.2. Fractional Anthracene Surface Coverage on Liquid Organic Aerosols. The amount of PAH surface coverage (i.e., the number of monolayers) has been shown to influence reaction rates.[5,12,13] Therefore, experiments were performed to determine the dependence of the anthracene surface coverage on the coating region temperature for both phenylsiloxane oil and azelaic acid aerosols. Both the phenylsiloxane oil and the azelaic acid aerosols are liquid and, as such, the anthracene may be found at the surface and in the bulk of the aerosol. If we assume that all the anthracene is at the aerosol surface, our values may be viewed as an upper limit to the surface coverage. The aerosols were sent through the anthracene coating region with temperatures ranging from 298 to 355 K, allowing us to control the anthracene surface coverage on the aerosols from submonolayer to greater than monolayer coverage. The slope of the least-squares plot of the anthracene surface concentration as a function of inverse temperature of the anthracene coating region (Figure 1) provided the sublimation enthalpy based on the Clausius−Clapeyron equation. In applying this equation, we assumed that the carrier gas in the anthracene coating region was saturated with anthracene vapor. We found experimental sublimation enthalpy values obtained in the experiments with phenylsiloxane oil and azelaic acid aerosols of 105 ± 4 and 117 ± 10 kJ mol^{-1}, respectively, which are in good agreement with the extrapolated literature value[21,22] of 104 kJ mol^{-1}. These values can be compared because the amount of anthracene these aerosols accumulate is proportional to the amount of anthracene in the gas phase which, in turn, is controlled by the sublimation of solid anthracene from the reservoir in the coating region. Assuming that anthracene is only found at the aerosol surface, all experiments were performed at a coverage of 0.3 monolayer, where 1 monolayer is defined as having a surface coverage of 10^{14} molecules cm^{-2} assuming spherical particles.

3.3. Kinetics of Surface-Bound Anthracene on Liquid Aerosols. The reaction of surface-bound anthracene on liquid phenylsiloxane oil and azelaic acid aerosols was investigated as a function of ozone concentration. Figure 2 displays plots of the anthracene surface concentration as a function of reaction time for this reaction on azelaic acid aerosols. The signals were normalized to constant aerosol number density. There was minimal change in the anthracene signal as a function of injector position with no ozone present. The reaction between surface-bound anthracene and ozone is well described by first-order kinetics given the linearity of the plots. The slope of the uncertainty-weighted linear-least-squares fit provided the pseudo-first-order rate coefficient (k^{I}_{obs}) at each ozone concentration studied. The uncertainty in this quantity was taken as the standard error in the slope of the plots at the 95% confidence interval.

The plot of k^{I}_{obs} as a function of flow tube ozone concentration (Figure 3) is nonlinear with a shape that is consistent with the Langmuir−Hinshelwood mechanism. The data in Figure 3

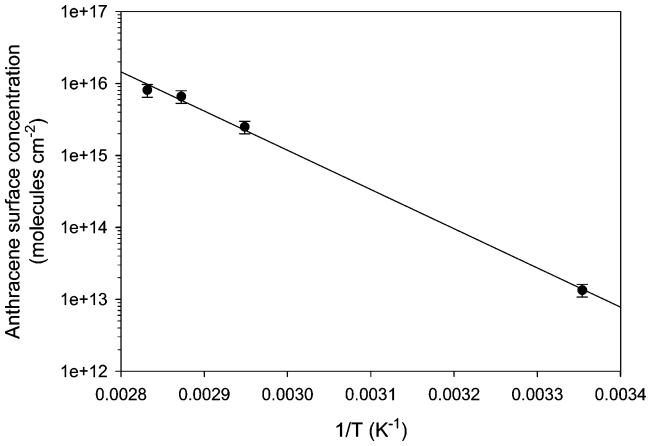

Figure 1. Anthracene surface coverage as a function of temperature of the anthracene coating region with phenylsiloxane oil as the aerosol substrate, assuming that anthracene is found only at the surface. A sublimation enthalpy of 105 kJ mol^{-1} was obtained, which is in excellent agreement with the extrapolated literature value[21,22] of 104 kJ mol^{-1}. In this study, the anthracene coating region temperature was 318 K.

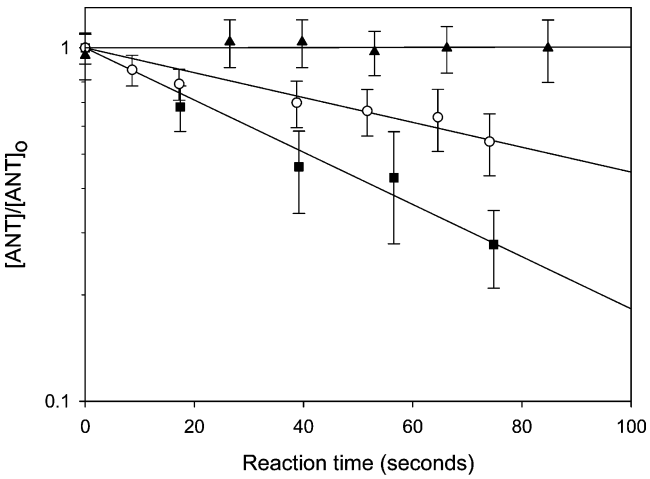

Figure 2. Kinetics of surface-bound anthracene and ozone under dry conditions on azelaic acid aerosols. The pseudo-first-order rate coefficients were determined from the slope of the uncertainty-weighted linear-least-squares fit for each ozone concentration. Symbols indicate ozone mixing ratios: filled triangles, no ozone; open circles, 5.8×10^{13} molecules cm^{-3}; filled squares, 1.9×10^{14} molecules cm^{-3}.

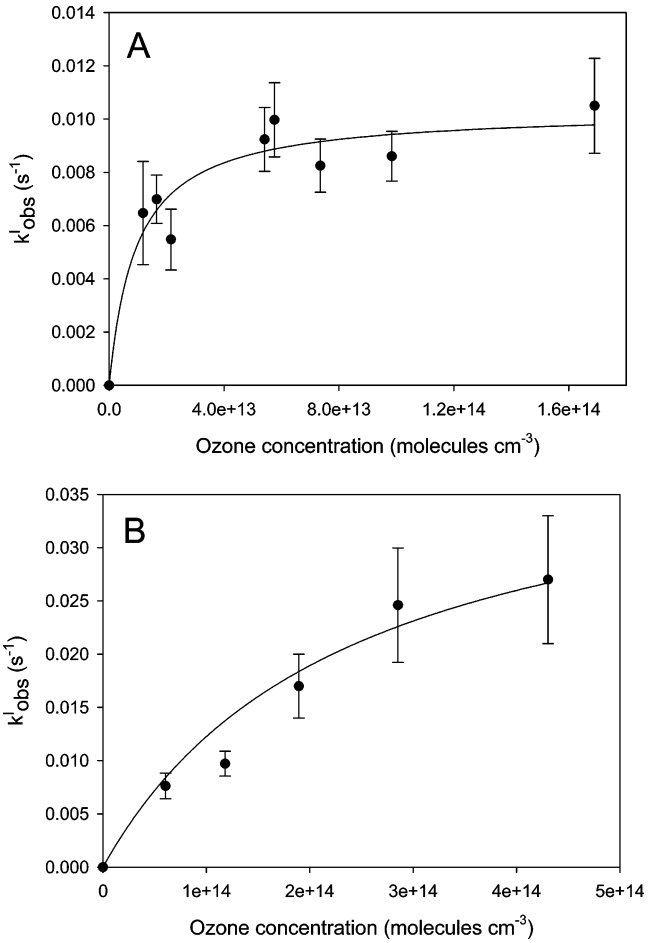

Figure 3. Pseudo-first-order rate coefficients (k^I_{obs}) as a function of gas-phase ozone concentration for the reaction of surface-bound anthracene and ozone on phenylsiloxane oil aerosols (A) and azelaic acid aerosols (B). The plots were fitted using a nonlinear-least-squares fit of eq 1. The standard error was obtained from the statistical error of the nonlinear-least-squares fit at the 95% confidence interval. The fitting parameters (K_{O_3} and k^I_{max}) for the reaction on both aerosol substrates are listed in Table 2.

were fitted using the following modified Langmuir−Hinshelwood equation:

$$k^I_{obs} = \frac{k^I_{max} K_{O_3} [O_{3(g)}]}{1 + K_{O_3} [O_{3(g)}]} \quad (1)$$

where k^I_{max} is the maximum rate coefficient that would be observed at high ozone concentrations, K_{O_3} is the ozone gas-to-surface equilibrium constant, and $[O_{3(g)}]$ is the gas-phase ozone concentration. The fitting parameters for the reaction of anthracene and ozone on azelaic acid and phenylsiloxane aerosols are summarized in Table 2. Although these experiments have been performed on liquid and supercooled aerosols and as such anthracene and ozone may diffuse into the bulk of the aerosol, based on our results, we believe that the reaction between anthracene and ozone proceeds at the surface. As discussed further in section 4.3, we believe that the large surface area to volume ratio and the short diffusion time from the bulk to the aerosol surface provide additional support that this reaction is occurring at the surface of both the liquid aerosol substrates.

3.4. Kinetic Experiments on Thin Films. There are a growing number of studies that have investigated the heterogeneous reactions of surface-bound PAHs on aerosol substrates,[5,6] at the air−aqueous interface[7,8] and on surface films.[9] However, as shown by looking at the kinetics of surface-bound anthracene and ozone, the surface-phase kinetics (i.e., k^I_{max}) of these reactions appear to be a factor of 10 faster on aerosol substrates compared to the kinetic experiments performed at the air−aqueous interface or on surface films, which were performed using a laser-induced-fluorescence setup. Therefore, we performed preliminary experiments of the kinetics of ozone and surface-bound anthracene on phenylsiloxane oil thin films using the laser-induced-fluorescence setup used by Kahan et al.[9] The goal was to study for the first time the same chemical system using the two general experimental approaches described in the recent literature.

The kinetic experiments on the thin films were performed at an ozone concentration of 10^{16} molecules cm^{-3} to determine the fastest kinetics of this reaction and measure k^I_{max}. To mimic how the PAH was deposited onto aerosols in the flow tube experiments, anthracene was deposited from the gas phase onto the phenylsiloxane oil thin film for either 1 or 3 min, which represents 0.1 or 0.6 anthracene monolayer on the surface of the film, respectively, if the PAH resides at the surface of the film. The amount of anthracene surface coverage was determined by extracting the phenylsiloxane thin film samples using offline analysis methods (refer to section 2.6). The kinetics of the reaction of surface-bound anthracene with ozone on phenylsiloxane oil thin films was first order with respect to anthracene. The pseudo-first-order rate constants for 1 and 3 min of anthracene deposition were $(2.1 \pm 0.3) \times 10^{-3}$ and $(9 \pm 1) \times 10^{-4}$ s^{-1}, respectively.

4. Discussion

4.1. Reaction Kinetics of Ozone and Anthracene on Azelaic Acid and Phenylsiloxane Aerosols. In agreement with our previous studies, the nonlinear plots of k^I_{obs} as a function of $[O_{3(g)}]$ (Figure 3) are consistent with a Langmuir−Hinshelwood reaction mechanism, where one reactant is strongly adsorbed to the surface and a second gas-phase reactant is in equilibrium between the gas phase and the surface. Thus, the reaction is a two-step process that involves the initial adsorption of the gas-phase reactant followed by a surface reaction. Our observations are in contrast to an Eley−Rideal reaction mechanism, which would have displayed a linear dependence of k^I_{obs} on $[O_{3(g)}]$.

One hypothesis of this study was that if the substrate governs the partitioning of ozone to the surface, then the K_{O_3} value should not depend on the PAH adsorbed to the surface. To test this, we investigated the reaction of surface-bound anthracene and ozone on azelaic acid aerosols to see if we would obtain results similar to our previous work looking at the kinetics of BaP and ozone on azelaic acid aerosol. The K_{O_3} values for the reaction of ozone with surface-bound anthracene and surface-bound BaP were $(2.2 \pm 0.9) \times 10^{-15}$ and $(1.2 \pm 0.4) \times 10^{-15}$ cm^3, respectively. Given that the K_{O_3} values vary over 2 orders of magnitude for the different substrates listed in Table 2, the results for anthracene and BaP on azelaic acid aerosols are quite similar and thus support our hypothesis. This similarity was also noted in Kahan et al.[9] This suggests that the K_{O_3} value reflects the partitioning behavior of ozone to the substrate irrespective of the PAH adsorbed to it. As shown in Table 2, the K_{O_3} values for the reaction of surface-bound anthracene with ozone on phenylsiloxane oil aerosols and azelaic acid aerosols are $(1.0 \pm 0.4) \times 10^{-13}$ and $(2.2 \pm 0.9) \times 10^{-15}$ cm^3, respectively. The K_{O_3} for azelaic acid is 2 orders of magnitude lower than that for the phenylsiloxane oil. However, the k^I_{max} for the two

TABLE 2: Comparison of Studies Investigating the Heterogeneous Reaction of Anthracene or BaP on Different Aerosol Substrates

	PAH	aerosol substrate	K_{O_3} (10^{-15} cm^3)	k^I_{max} (s^{-1})
Pöschl et al.[5]	BaP	soot	280 ± 20	0.015 ± 0.001
Kwamena et al.[6]	BaP	azelaic acid	1.2 ± 0.4	0.048 ± 0.008
this study	anthracene	phenylsiloxane oil	100 ± 40	0.010 ± 0.003
		azelaic acid	2.2 ± 0.9	0.057 ± 0.009

substrates only vary by a factor of 3. The similarity of the k^I_{max} values for the different systems listed in Table 2 implies that once ozone is on the aerosol surface, irrespective of the identity of the PAH involved in the reaction, there is an inherent barrier to the reaction that results in similar k^I_{max} values. We suggest that this barrier may be due to the diffusion mobility of the two reactants on the aerosol surface or instead that it is related to a rate-determining transformation that ozone must undergo on the surface, which is required for reaction to occur. We now discuss each possibility in more detail.

After ozone partitions to the aerosol surface, the two reactants must be in close enough proximity for a reaction to occur; i.e., it is possible that the mobility of the reactants restricts the rate at which they can react, in the form of a diffusion-controlled surface reaction.[15] The magnitude of such a diffusion-controlled rate constant is not easy to estimate. While this mobility constraint sets the overall magnitude of the value of k^I_{max}, we also see some evidence that the interaction between ozone and the substrate may play a role in the availability of ozone to participate in the reaction. In particular, from Table 2, there is a suggestion that higher K_{O_3} values result in smaller k^I_{max} values and therefore increased partitioning of ozone to the aerosol substrate may make the ozone less available for reaction with the surface-bound PAH, because of reduced mobility.

Another possibility is that this barrier may arise from ozone being transformed into a more reactive form prior to reaction with the PAH, via a process such as ozone decomposition. Ozone decomposition has been suggested in an analogous manner on a wide range of systems including Saharan dust,[23,24] alumina,[25,26] and soot.[27,28] If the barrier to the transformation on each substrate is similar, then the values for k^I_{max} should also be similar in each of these systems. Indeed, kinetic analysis of the results from our laboratory for the loss of ozone on Saharan dust[24] and on alumina[25] are both consistent with k^I_{max} values between 10^{-3} and 10^{-2} s^{-1}, which is not dissimilar to the values obtained in this work. Based on our results, we cannot determine which explanation for the barrier is the more likely one.

To extend the prevalence of this mechanism, we note that Langmuir−Hinshelwood behavior has also been observed in the reaction of ozone with other compounds such as unsaturated self-assembled monolayers (SAMs)[29] and internal mixtures of sodium oleate and aqueous NaCl droplets.[30] McNeill et al. obtained a best-fit k^I_{max} value of 0.05 s^{-1} in their study investigating the multiphase reaction of ozone with sodium oleate (a proxy for oleic acid) coated on NaCl droplets. This value is very similar to the k^I_{max} values listed in Table 2 for the reaction of surface-bound PAHs and ozone.

In our previous work,[6] we compared the K_{O_3} values for the different substrates that had been investigated to date and we proposed that ozone prefers partitioning to nonpolar surfaces. As shown in Table 3, soot, which is nonpolar, has the highest K_{O_3} value compared to the polar aqueous substrate with the lowest. The phenylsiloxane oil used in this study is nonpolar given the many phenyl and methyl functional groups, and therefore the K_{O_3} value observed for this substrate is in agreement with our suggestion of increased partitioning of ozone to nonpolar surfaces. The ozone equilibrium constant values for the SAM/ozone system and the oleate/aqueous NaCl/ozone system were 2.5×10^{-14} and 4.0×10^{-14} cm^3, respectively.[29,30] These values fall within the range of equilibrium constants listed in Table 3 and suggest that the partitioning of ozone to these surfaces is greater than the partitioning of ozone to azelaic acid aerosols but less than the partitioning of ozone to soot or phenylsiloxane oil aerosols.

Another example that illustrates that ozone prefers partitioning to nonpolar surfaces is provided by the molecular dynamic simulations by Vieceli et al.[31] In their simulations of the interaction between ozone and a phospholipid monolayer and ozone and a self-assembled monolayer, the residence time of ozone on the phospholipid monolayer was greater. The ozone only remained in the nonpolar lipid portion of the phospholipid monolayer and did not penetrate the aqueous region. The lower solubility of ozone in water compared to organic liquids has been suggested as a possible explanation. Donaldson et al.[32] estimated a K_{oa} value of 20 for ozone in 1-octanol. We estimate a K_{aw} of 4×10^{-4} based on a Henry's law constant of 0.011 mol L^{-1} atm^{-1}.[33] A comparison of these estimated parameters provides additional support as to why ozone prefers partitioning to nonpolar surfaces.

4.2. Quantum Calculations. Computational calculations were performed as a preliminary means of investigating if the differences in the energy of interaction of the different substrates with ozone could begin to explain the observed trends in the K_{O_3} values. DFT calculations were used to determine the binding energy of the ozone−substrate complex that forms when O_3 initially partitions to the surface. We anticipated that the ozone−substrate complex binding energies may mimic the trend of the K_{O_3} values for the different substrates investigated. We compared our results of the binding energy of the water−ozone complex with studies found in the literature. This was the only complex examined for which other computational results could be found in the literature. We calculated a binding energy of 0.69 kcal mol^{-1} for the water−ozone complex. Tachikawa and Abe[34−36] calculated binding energies ranging from 0.63 to 3.58 kcal mol^{-1} using both ab initio and DFT calculations for the water−ozone complex. It should be noted that Tachikawa and Abe only included zero-point and BSSE corrections in their most recent study[36] for which they calculated binding energies of 1.51 and 0.64 kcal mol^{-1} for two different forms of the water−ozone complex. Their results are in reasonable agreement with ours.

TABLE 3: Comparison of K_{O_3} Values for Different Substrates for Which the Surface Reaction Has Been Observed To Proceed by the Langmuir−Hinshelwood Mechanism

study	substrate	K_{O_3} (10^{-15} cm^3)
Pöschl et al.[5]	soot aerosols	280
this study	phenylsiloxane oil aerosols	100
McNeill et al.[30]	aqueous NaCl droplets	40
Dubowski et al.[29]	self-assembled monolayers	25
this study	azelaic acid aerosols	2.2
Kahan et al.[9]	octanol thin films	0.56
Mmereki et al.[7]	water	0.466

TABLE 4: Summary of k^{I}_{max} and K_{O_3} Values for the Heterogeneous Reaction of Anthracene and Ozone on Different Aerosol and Thin Film Surfaces

	substrate	K_{O_3} (10^{-15} cm^3)	k^{I}_{max} (s^{-1})
this study	phenylsiloxane oil aerosols	100	0.010
	phenylsiloxane oil thin film		0.002
Kahan et al.[9]	octanol thin film	0.56	0.002
Mmereki et al.[7]	water	0.466	0.0026

The calculated binding energies for the azelaic acid−ozone, octanol−ozone, and water−ozone complexes were 2.22, 1.10, and 0.69 kcal mol^{-1}, respectively, mimicking the trend of the K_{O_3} values for these substrates. The ozone interacts with the OH functionalities of azelaic acid, octanol, and water. However, there are no OH functionalities on benzene, and as such the calculated interaction between benzene and ozone is somewhat weaker than that of the other substrates. Our calculated benzene−ozone binding energy was 0.35 kcal mol^{-1}. We suspect that the benzene−ozone electronic interaction may be more complex than that represented in our calculations, and this is why the binding energy does not follow the trend for the K_{O_3} values. In particular, we used single electronic configurations in this work, whereas there is the potential for substantial charge exchange in a system of this type. Nelander and Nord[37] performed an absorption spectroscopy study investigating different ozone−olefin complexes, including ozone−benzene, at low temperatures and observed a charge-transfer complex between ozone and benzene. This might strengthen the binding energy estimate between ozone and benzene if it were included. This preliminary work suggests that the binding energy may begin to explain the different partitioning behaviors ozone has toward different substrates. However, future studies that more accurately capture the ozone−substrate as well as the ozone−PAH complex are required. These calculations are beyond the scope of this present work.

4.3. Comparison of Kinetics on Aerosol and Thin Film Surfaces. The kinetics of surface-bound anthracene with ozone are a factor of 10 times faster on aerosol substrates[5,6] compared to on thin films[9] and or at the air−aqueous interface.[7,8] We performed experiments looking at the reaction of surface-bound anthracene with ozone on phenylsiloxane thin films in order to study the same chemical system using the two general experimental approaches described in the literature. As shown in Table 4, the substrate used does not account for the differences between the two approaches.

By examining both arguments for and against, we explore below whether liquid diffusion constraints might provide an explanation to this discrepancy. We found that the amount and location of anthracene along with the time for diffusion in the thin film experiments were consistent with diffusion being a limiting factor in the kinetics. However, the similarities in the k^{I}_{max} values for the reaction of surface-bound anthracene with ozone at the air−aqueous interface,[7] on octanol-coated water surfaces,[7,8] and on 1-octanol thin films[9] suggest that diffusion may not fully explain the differences between the two experimental approaches and, as such, the difference remains an open question that requires further investigation. The following discussion expands in detail upon the arguments both in favor and against liquid-phase diffusion accounting for the differences.

The following questions were asked to determine the importance of diffusion in the thin film and aerosol experiments:

(1) Where is the anthracene located in the thin film experiments?

Analysis of the adsorption isotherm presented in the study by Kahan et al.[9] provides further insight on the partitioning of anthracene between the surface and the bulk in the film experiments. We assumed that the plateau of the adsorption isotherm in Figure 5 of Kahan et al.[9] corresponds to a monolayer of anthracene surface coverage. The anthracene in octanol concentration at the start of the plateau or the monolayer regime corresponds to approximately 10^{-4} M. In most experiments presented by Kahan et al.,[9] solutions of 10^{-5} M anthracene in octanol were used, which according to the adsorption isotherm corresponds to 1/10 monolayer, i.e., 1×10^{13} molecules cm^{-2}, assuming that a monolayer corresponds to 1×10^{14} molecules cm^{-2}. However, given the amount of the 10^{-5} M solution that was used and assuming all the anthracene was at the surface of the thin film, the anthracene surface concentration would be approximately 7×10^{13} molecules cm^{-2}. This value is 7 times what the adsorption isotherm indicates is at the surface at this anthracene concentration, and therefore, considering the high K_{oa} value for anthracene and assuming that the partitioning of anthracene between octanol and air would be similar to the partitioning of anthracene between phenylsiloxane oil and air, any excess anthracene should be found in the bulk of the film.

(2) What is the time for anthracene diffusion in the particle and thin film experiments?

The time scales for diffusion in the particles and in the films are estimated to be 1×10^{-5} and 110 s, respectively,[4,38] where the diffusion coefficient for anthracene in phenylsiloxane oil was assumed to be 10^{-6} cm^2 s^{-1} based on an estimated diffusion coefficient of ozone in organic acids, such as oleic acid.[39] If the time for diffusion in the thin film was assumed to be the e-folding time for the reaction, the pseudo-first-order rate constant would be approximately 9×10^{-3} s^{-1}, which is similar in magnitude to the k^{I}_{max} values for the studies by Donaldson and co-workers[7−9] and in this work for the phenylsiloxane thin films.

This analysis suggests that most of the anthracene is in the bulk in the thin film experiments so that any anthracene depleted at the surface must be replenished by diffusion from the bulk. The time for diffusion may make the kinetic measurements in the thin film experiments diffusion limited. However, there are also arguments that can be made against diffusion as an explanation.

In the studies by Mmereki et al.,[7,8] experiments were performed at the air−aqueous interface on thick water surfaces. However, the solubility of anthracene in water is very low and as such one would only expect anthracene to be found at the air−aqueous interface. Liquid diffusion should not play a role in the kinetics since very little anthracene should be found in the bulk. Subsequent work by Donaldson and co-workers on octanol-coated aqueous surfaces[8] and on thin films[9] has determined k^{I}_{max} values similar to those determined for the same reaction at the air−aqueous interface.[7,8] The similarity in the k^{I}_{max} values on these different substrates suggests that the reaction of surface-bound anthracene with ozone on thin film surfaces proceeds by the same mechanism and that the kinetics are not diffusion limited in these later experiments. Furthermore, if the thin film experiments by Kahan et al.[9] were diffusion limited, the k^{I}_{max} values should be similar for the six PAHs investigated, since it is not expected that the diffusion coef-

TABLE 5: PAH Lifetimes on Different Aerosol Substrates and Thin Film Surfaces at an Ozone Concentration of 50 ppb

study	PAH	substrate	lifetime
Pöschl et al.[5]	BaP	soot aerosols	4 min
Kwamena et al.[6]		azelaic acid aerosols	4 h
this study		phenylsiloxane oil aerosols	14 min
		azelaic acid aerosols	1.3 h
Kwamena et al.[15]	anthracene	Pyrex	13 h
Kahan et al.[9]		octanol thin film	8.4 days
Mmereki et al.[8]		water	7.9 days

ficients for the different PAHs would vary over an order of magnitude in the way the k^{I}_{max} values reported by Kahan et al.[9] do.

These arguments suggest that diffusion alone cannot reconcile the differences in the kinetics results obtained between the two experimental approaches. We feel that this difference requires further study to determine the insight it may give us into the factors that govern heterogeneous reactions.

5. Atmospheric Implications and Conclusions

In this study we sought to improve our understanding of how the aerosol substrate influences heterogeneous reactions. Consistent with the initial study of Pöschl et al.,[5] we have shown that the reaction of surface-bound anthracene and ozone does proceed by the Langmuir−Hinshelwood mechanism for the substrates investigated. Based on the recent body of work investigating heterogeneous reactions of PAHs and ozone on aerosol surfaces,[5,6] proxies for aerosol surfaces,[15] at the air−aqueous interface,[7,8] and on surface films,[9] it seems generally accepted that these heterogeneous reactions proceed by the Langmuir−Hinshelwood mechanism.

One of our goals was to determine if the ozone equilibrium constant is a parameter that describes the partitioning of ozone to the aerosol substrate irrespective of the species adsorbed to it. If so, we hypothesized that the K_{O_3} values in our studies with surface-bound BaP and surface-bound anthracene should be similar. Indeed, we did observe similar K_{O_3} values for these different PAHs. We further propose that higher K_{O_3} values are due to stronger binding interactions of the initial ozone−substrate complex, as tentatively shown by our preliminary investigations using ab initio calculations. We also noted that the k^{I}_{max} values for different PAHs on the same surface were similar. We postulate that this similarity is because of a common rate-determining step in each reaction. This barrier may be related to mobility that allows the two reactants to be in close enough proximity for a reaction to occur, or the barrier may arise from the transformation of ozone into a more reactive form on the substrate's surface.

We also performed a preliminary comparison between the kinetic results obtained from studies on aerosol substrates and thin films, finding faster kinetics on the particles. Condensed-phase diffusion could not fully reconcile the difference between the two types of experiments. Further studies are required in this regard.

The faster rates on particle surfaces suggest that these reactions may be an important sink for PAHs in highly polluted areas, as shown in a recent modeling study.[11] Further, the lifetime of these species may be highly dependent on the aerosol substrate. As Table 5 illustrates, the lifetime of anthracene ranges from 14 min on substrates chemically similar to phenylsiloxane oil to approximately 8 days on water surfaces. Therefore, the aerosol substrate must be considered to accurately model the reactive fate of PAHs. However, the reaction of PAHs with ozone is only one heterogeneous reactive loss mechanism. Heterogeneous reactions with OH, NO_3, and N_2O_5 may also be important loss processes. Very little work has been done in this regard.

Acknowledgment. We thank Scott Mabury and Joyce Dinglasan-Panlilio for use and help with the HPLC−UV−vis and Dan Mathers of the ANALEST facility for use of the HPLC-fluorescence instrument. We thank Jeff McCabe for performing the low-pressure, coated-wall flow tube experiments. We also thank an anonymous reviewer for valuable comments. Acknowledgment is made to the donors of the Petroleum Research Fund, administered by the American Chemical Society, for support of this work, as well as to NSERC. N.-O.A.K. also thanks NSERC for the award of a PGS D Scholarship.

References and Notes

(1) Rudich, Y. *Chem. Rev.* **2003**, *103*, 5097.
(2) Saxena, P.; Hildemann, L. M. *J. Atmos. Chem.* **1996**, *24*, 57.
(3) Atkinson, R.; Arey, J. *Environ. Health Perspect.* **1994**, *102*, 117.
(4) Finlayson-Pitts, B. J.; Pitts, J. N., Jr. *Chemistry of the Upper and Lower Atmosphere*; Academic Press: Toronto, 2000.
(5) Poschl, U.; Letzel, T.; Schauer, C.; Niessner, R. *J. Phys. Chem. A* **2001**, *105*, 4029.
(6) Kwamena, N.-O. A.; Thornton, J. A.; Abbatt, J. P. D. *J. Phys. Chem. A* **2004**, *108*, 11626.
(7) Mmereki, B. T.; Donaldson, D. J. *J. Phys. Chem. A* **2003**, *107*, 11038.
(8) Mmereki, B. T.; Donaldson, D. J.; Gilman, J. B.; Eliason, T. L.; Vaida, V. *Atmos. Environ.* **2004**, *38*, 6091.
(9) Kahan, T. F.; Kwamena, N.-O. A.; Donaldson, D. J. *Atmos. Environ.* **2006**, *40*, 3448.
(10) Mak, J.; Gross, S.; Bertram, A. K. *Geophys. Res. Lett.* **2007**, *34*, Article No. L10804.
(11) Kwamena, N. O. A.; Clarke, J. P.; Kahan, T. F.; Diamond, M. L.; Donaldson, D. J. *Atmos. Environ.* **2007**, *41*, 37.
(12) Alebic-Juretic, A.; Cvitas, T.; Klasinc, L. *Environ. Sci. Technol.* **1990**, *24*, 62.
(13) Wu, C.-H.; Salmeen, I.; Niki, H. *Environ. Sci. Technol.* **1984**, *18*, 603.
(14) Adamson, A. W. *Physical Chemistry of Surfaces*, 5th ed.; John Wiley and Sons: Toronto, 1990.
(15) Kwamena, N.-O. A.; Earp, M. E.; Young, C. J.; Abbatt, J. P. D. *J. Phys. Chem. A* **2006**, *110*, 3638.
(16) Brown, R. L. *J. Res. Natl. Bur. Stand.* **1978**, *83*, 1.
(17) Hearn, J. D.; Smith, G. D. *Phys. Chem. Chem. Phys.* **2005**, *7*, 2549.
(18) Braban, C. F.; Carroll, M. F.; Styler, S. A.; Abbatt, J. P. D. *J. Phys. Chem. A* **2003**, *107*, 6594.
(19) Cziczo, D. J.; Nowak, J. B.; Hu, J. H.; Abbatt, J. P. D. *J. Geophys. Res.* **1997**, *102*, 18843.
(20) Frisch, M. J.; Trucks, G. W.; Schlegel, H. B.; Scuseria, G. E.; Robb, M. A.; Cheeseman, J. R.; Montgomery, J. A., Jr.; Vreven, T.; Kudin, K. N.; Burant, J. C.; Millam, J. M.; Iyengar, S. S.; Tomasi, J.; Barone, V.; Mennucci, B.; Cossi, M.; Scalmani, G.; Rega, N.; Petersson, G. A.; Nakatsuji, H.; Hada, M.; Ehara, M.; Toyota, K.; Fukuda, R.; Hasegawa, J.; Ishida, M.; Nakajima, T.; Honda, Y.; Kitao, O.; Nakai, H.; Klene, M.; Li, X.; Knox, J. E.; Hratchian, H. P.; Cross, J. B.; Adamo, C.; Jaramillo, J.; Gomperts, R.; Stratmann, R. E.; Yazyev, O.; Austin, A. J.; Cammi, R.; Pomelli, C.; Ochterski, J. W.; Ayala, P. Y.; Morokuma, K.; Voth, G. A.; Salvador, P.; Dannenberg, J. J.; Zakrzewski, V. G.; Dapprich, S.; Daniels, A. D.; Strain, M. C.; Farkas, O.; Malick, D. K.; Rabuck, A. D.; Raghavachari, K.; Foresman, J. B.; Ortiz, J. V.; Cui, Q.; Baboul, A. G.; Clifford, S.; Cioslowski, J.; Stefanov, B. B.; Liu, G.; Liashenko, A.; Piskorz, P.; Komaromi, I.; Martin, J. M.; Fox, D. J.; Keith, T.; Al-Laham, M. A.; Peng, C. Y.; Nanayakkara, A.; Challacombe, M.; Gill, P. M. W.; Johnson, B.; Chen, W.; Wong, M. W.; Gonzalez, C.; Pople, J. A. *Gaussian 03*, revision B.03; Gaussian Inc.: Pittsburgh, 2003.
(21) *Spectral Atlas of Polycyclic Aromatic Compounds*; Kluwer Academic Publishers: Boston, 1998; Vol. 2.
(22) De Kruif, C. G. *J. Chem. Thermodyn.* **1980**, *12*, 243.
(23) Hanisch, F.; Crowley, J. N. *Atmos. Chem. Phys.* **2003**, *3*, 119.
(24) Chang, R. Y.-W.; Sullivan, R. C.; Abbatt, J. P. D. *Geophys. Res. Lett.* **2005**, *32*, L14815.
(25) Sullivan, R. C.; Thornberry, T.; Abbatt, J. P. D. *Atmos. Chem. Phys.* **2004**, *4*, 1301.
(26) Alebic-Juretic, A.; Cvitas, T.; Klasinc, L. *Environ. Monit. Assess.* **1997**, *44*, 241.

(27) Disselkamp, R. S.; Carpenter, M. A.; Cowin, J. P.; Berkowitz, C. M.; Chapman, E. G.; Zaveri, R. A.; Laulainen, N. S. *J. Geophys. Res.* **2000**, *105*, 9767.

(28) Kamm, S.; Mohler, O.; Naumann, K.-H.; Saathoff, H.; Schurath, U. *Atmos. Environ.* **1999**, *33*, 4651.

(29) Dubowski, Y.; Vieceli, J.; Tobias, D. J.; Gomez, A.; Lin, A.; Nizkorodov, S. A.; McIntire, T. M.; Finlayson-Pitts, B. J. *J. Phys. Chem. A* **2004**, *108*, 10473.

(30) McNeill, V. F.; Wolfe, G. M.; Thornton, J. A. *J. Phys. Chem. A* **2007**, *111*, 1073.

(31) Vieceli, J.; Ma, O. L.; Tobias, D. J. *J. Phys. Chem. A* **2004**, *108*, 5806.

(32) Donaldson, D. J.; Mmereki, B. T.; Chaudhuri, S. R.; Handley, S.; Oh, M. *Faraday Discuss.* **2005**, *130*, 227.

(33) Seinfeld, J. H.; Pandis, S. N. *Atmospheric Chemistry and Physics*; John Wiley and Sons: New York, 1998.

(34) Tachikawa, H.; Abe, S. *Inorg. Chem.* **2003**, *42*, 2188.

(35) Tachikawa, H.; Abe, S. *Inorg. Chim. Acta* **2005**, *358*, 288.

(36) Tachikawa, H.; Abe, S. *Chem. Phys. Lett.* **2006**, *432*, 409.

(37) Nelander, B.; Nord, L. *J. Am. Chem. Soc.* **1979**, *101*, 3769.

(38) Atkins, P. W. *Physical Chemistry*, 2nd ed.; Oxford University Press: Toronto, 1982.

(39) Moise, T.; Rudich, Y. *J. Phys. Chem. A* **2002**, *106*, 6469.